Multi-Functional Dual-Layer Polymer Electrolytes for Lithium Metal Polymer Batteries

Young-Gi Lee, Kwang Sun Ryu, and Soon Ho Chang

We prepared a novel multi-functional dual-layer polymer electrolyte by impregnating the interconnected pores with an ethylene carbonate (EC)/dimethyl carbonate (DMC)/lithium hexafluorophosphate (LiPF$_6$) solution. The first layer, based on a microporous polyethylene, is incompatible with a liquid electrolyte, and the second layer, based on poly (vinylidenefluoride-co-hexafluoropropylene), is submicroporous and compatible with an electrolyte solution. The maximum ionic conductivity is 7×10^{-3} S/cm at ambient temperature. A unit cell using the optimum polymer electrolyte showed a reversible capacity of 198 mAh/g at the 500th cycle, which was about 87% of the initial value.

Keywords: Dual-layer polymer electrolyte, lithium anode, compatibility, morphology, ionic conductivity, capacity.

I. Introduction

As information and telecommunication technologies develop, ubiquitous devices such as third-generation wireless communication systems and next-generation PCs or PDAs will require advanced mobile power sources having high energy and power densities. One candidate is a lithium metal polymer battery (LMPB) using a lithium (Li) metal anode and a polymer electrolyte [1], [2].

Although theoretically the most promising, LMPBs have encountered difficulties for commercialization because of their poor safety and cycle performance. These problems are associated with the reactivity of Li anodes, the growth of dendrites, and dead Li formation at the anode surface upon cycling [3]-[5]. The penetration growth of dendrites through an electrolyte film is mainly responsible for a short-circuit during the charging stage, and Li^0 powders stripped from the dendritic anode surface into the electrolyte solution during the discharging stage can lead to an explosion or fire when exposed to humid conditions. Thus, the uniform Li$^+$-plating issue on the Li-anode surface during the charging process is the key point to overcome these problems.

For the past two decades, there have been various attempts to improve the safety and cyclability of LMPBs by developing manifold solvent-free and manifold plasticized polymer electrolytes [6]-[11]. However, they still have performance limits such as a low ionic conductivity at ambient temperature and poorer mechanical properties than separator/liquid electrolyte systems in lithium-ion batteries.

In this study, we have introduced a novel multi-functional polymer electrolyte having a dual-layer film structure comprised of an initial porous polymer film with micron-scaled pores based on polyethylene (PE) and a secondary porous
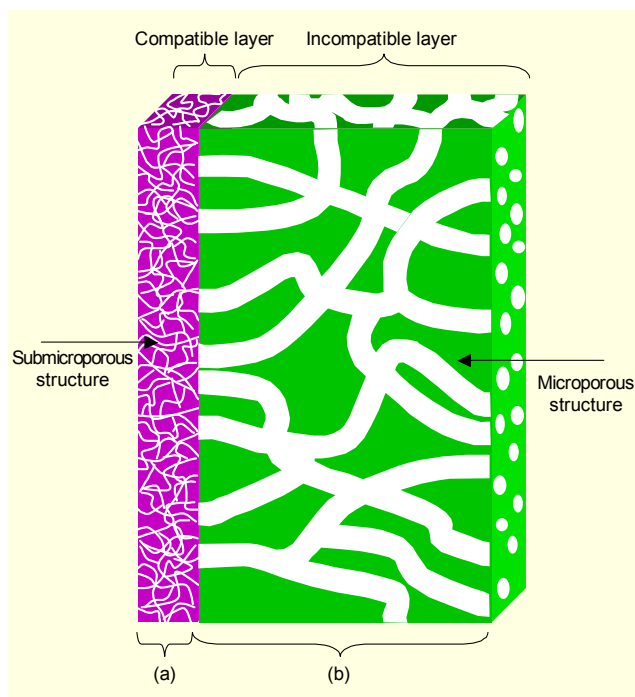
Fig. 1. The schematic feature of the dual-layer membrane system: (a) submicroporous P(VdF-co-HFP) and (b) microporous PE.

polymer film with submicron-scaled pores based on poly(vinylidenefluoride-co-hexafluoropropylene) (P(VdF-co-HFP)) coated on the surface of the first porous polymer film, both of which are shown in Fig. 1.

The microporous PE, the first layer (b) in Fig. 1, acts only as a structural support, while channels filled with a liquid electrolyte work as a conducting pathway such as in a separator/liquid electrolyte system. The second layer, (a) in Fig. 1, makes contact with the Li-anode surface to effectively control the dendritic growth and surface morphology of the anode.

To control the reaction site of Li^+ on the surface, we designed a homogeneous electrolyte zone near the Li-anode surface by choosing a relevant matrix polymer having compatibility with the liquid electrolytes. We investigated the ionic conductivities of polymer electrolytes as a function of the thickness of the second layer and the uptake amount of the liquid electrolyte. We also investigated the charge/discharge cycling behavior of a unit cell.

II. Experimental

1. Preparation of Polymer Electrolytes

The appropriate amount of P(VdF-co-HFP) and silanized fumed silica were completely dissolved and dispersed in acetone after being homogenized for 24 hours in a laboratory ball mill. The viscous solution was coated on the surface of a PE membrane (Asahi Kasei with a thickness of 25 μm and a 40% porosity) using a doctor blade. The films were impregnated with a liquid electrolyte solution (1M $LiPF_6$ in EC/DMC (1/1, w/w)).

2. Sample Characterization

We observed a cross-sectional morphology of the dual-layer membranes using a scanning electron microscope (Philips SEM 535M) and optical images of the polymer electrolyte surface using a digital camera (COOLPIX995, Nikon).

3. Electrochemical Characterization

We measured the impedance of the specimen over a frequency range of 100 Hz to 10 MHz using the Solartron 1255 frequency response analyzer. The cathode was prepared by coating the slurry, made up of an 80%-Li[$Ni_{0.15}Li_{0.23}Mn_{0.62}$]$O_2$ powder synthesized by a simple combustion method [12], [13], a 12%-super-P carbon, and an 8%-PVdF binder, onto aluminum foil. We fabricated a unit cell by sandwiching the dual-layer polymer electrolyte between a Li-metal anode and the cathode. The charge/discharge cycling test of the cell was conducted galvanostatically using battery testing equipment (TOSCAT-3000U) between 2.0 and 4.8 V with a current density of 0.5 mA/cm^2.

III. Results and Discussion

1. Cross-Sectional Structure of a Dual-Layer Membrane

Figure 2 reveals the typical SEM images of cross-sections of dual-layer membranes.

The lower layer is the first layer based on a PE membrane with a thickness of 25 μm. The upper layer is the second layer based on P(VdF-co-HFP), which is coated onto the surface of the first layer as a function of concentration of the polymer in the coating slurry. The thickness of the coated (second) layer increases as the polymer concentration in the coating slurry increases. As observed in (a) through (d) of Fig. 2 and shown in Table 1, the thickness of the coated layer ranged from 0.9 to 18 μm.

Large and well-developed micropores were found in the PE layer, as (f) in Fig. 2 shows, while the randomly connected submicropores were observed in the coated layer, which (e) in Fig. 2 illustrates. These structural differences of the two layers result from the use of different polymeric materials and manufacturing processes. The PE film is manufactured by calendering the PE melt; thus the micropores become rather distorted and flat during the roll-pressing process. The P(VdF-co-HFP) layer is coated using a polymer slurry. As the casting
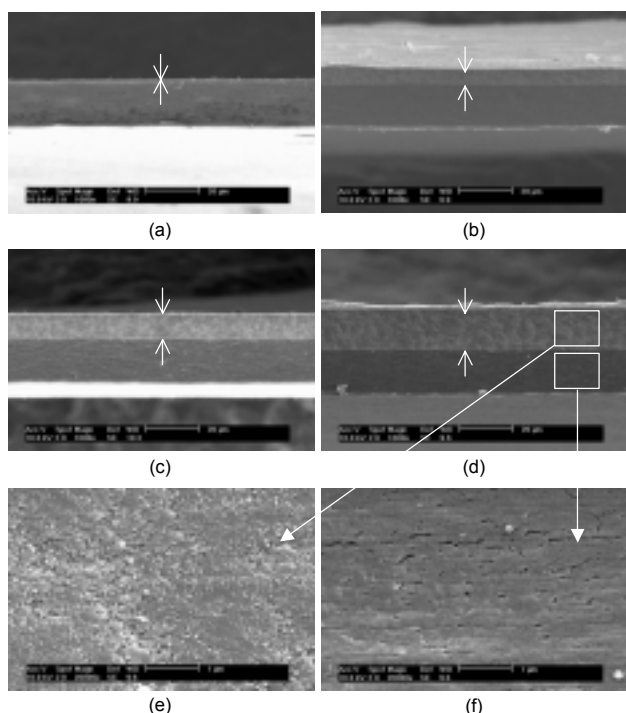
Fig. 2. SEM images of the cross-section of the duay-layer membranes prepared as a function of polymer concentration in the coating slurry: (a) 2 wt%, (b) 5 wt%, (c) 10 wt%, (d) 15 wt% (×1,000), (e) enlarged (×20,000) region of the upper layer, and (f) enlarged region of the lower layer.

Table 1. The thickness of the coated layer and dual-layer membrane.

Polymer conc. (wt%)	2	5	10	15
Coated layer (μm)	0.9	6	11	18
Dual-layer membrane (μm)	25.9	31	36	43

solvent evaporates, the polymer fibrils are connected and the pore space is generated through the amorphous regions located near the grain boundaries of the compacted crystalline dominant phases. Some of the added silica partially disrupted the crystalline phases, which made the regional crystalline dominant phases much smaller. Thus, a smaller pore space is generated near the grain boundaries [14], [15].

2. Uptake of Liquid Electrolytes

Figure 3 shows optical micrographs of the surfaces of the dual-layer polymer electrolyte and bare PE membrane after soaking in liquid electrolyte for 3 hours.

The coated surface of the dual-layer polymer electrolyte is almost homogeneous, as shown in Fig. 3(a). This might be due
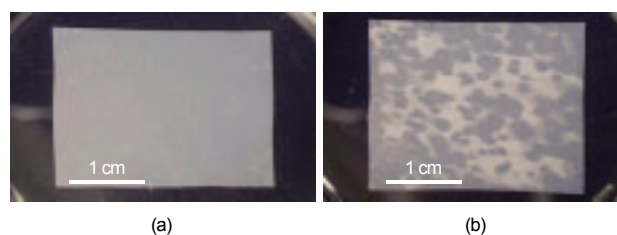

Fig. 3. Optical micrographs of (a) the coated surface of the dual-layer polymer electrolyte surface (0.9 μm coated) and (b) the bare PE membrane/liquid electrolyte surface after an uptake of liquid electrolytes.
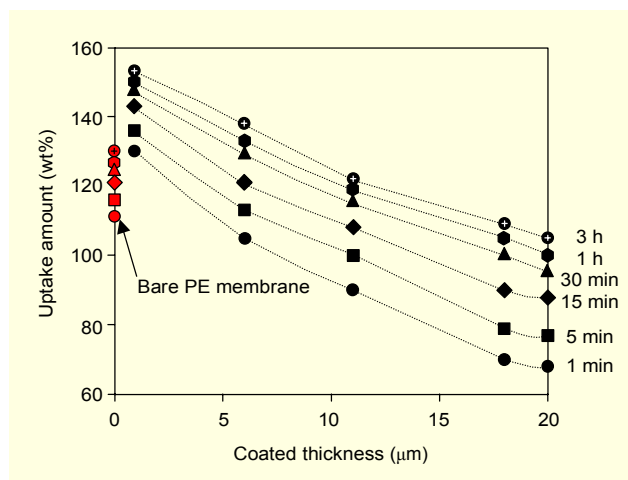

Fig. 4. The uptake amount of liquid electrolytes into dual-layer membranes as a function of their coated-layer thicknesses at different soaking times.

to the formation of a homogeneous electrolyte zone within the coated layer through the enhanced compatibility between the matrix polymer of P(VdF-co-HFP) and the liquid electrolytes. However, the bare PE membrane/liquid electrolyte system, shown in Fig. 3(b), shows an inhomogeneous surface. The bright areas correspond to non-porous crystalline PE regions, which are the least swollen with liquid electrolytes and have a very dense morphology. The dark regions correspond to the electrolyte-rich phases within the porous structures and the amorphous PE regions swollen with liquid electrolytes.

Figure 4 shows the uptake amount of liquid electrolytes into the dual-layer membranes having various coating layer thicknesses. For comparison, the electrolyte uptake of a bare microporous PE membrane (red symbols) was also investigated.

The initial uptake within the first 15 min. reflects the selective filling of micro- and submicropores within the matrix by a liquid electrolyte. The further gradual increase of the uptake with respect to soaking time can be explained by the swelling of the amorphous PE matrix due to the saturation of

the electrolyte into the free volumes among the polymer chains or fibrils. The uptake reaches its maximum point at a coating thickness of 0.9 μm for each soaking time. Thus, we confirmed that the low wettability problem for the non-polar PE polymer can be improved by introducing another layer based on a P(VdF-co-HFP)/silanized fumed silica composite, which has compatibility with the liquid electrolytes owing to the interaction between the fluorine group within the polymer chain or silica and an organic solvent in the liquid electrolytes [16], [17]. However, the electrolyte uptake decreases with an increase in the coating thickness, probably because an overly-thick coating inhibits the electrolyte permeation into the porous PE membrane from the coated side.

3. Apparent Ionic Conductivity of Polymer Electrolytes

Figure 5 illustrates the apparent ionic conductivity of the dual-layer polymer electrolytes as a function of coated thickness at different soaking periods. The 0.9-μm coated membrane shows the highest ionic conductivity of 7.0×10^{-3} S/cm at ambient temperature after soaking for 3 hours. The apparent conductivity becomes lower as the coated thickness increases. For reference, the bare PE membrane/liquid electrolyte system shows a maximum ionic conductivity of 5.8×10^{-3} S/cm under the same conditions.
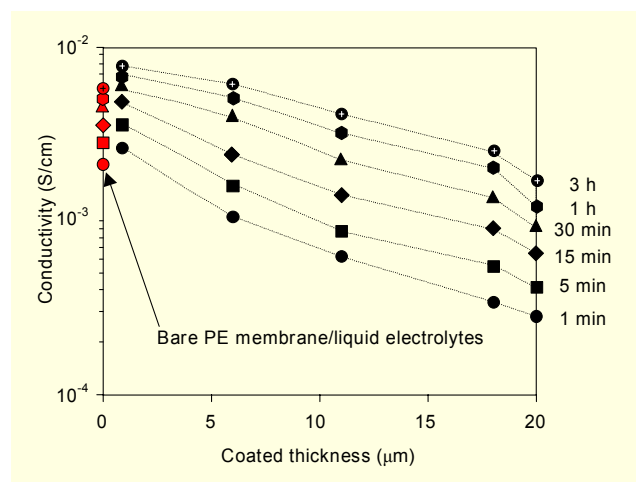

Fig. 5. Apparent ionic conductivity of the dual-layer polymer electrolytes as a function of coated thickness at different soaking periods.

The observed conductivity depends primarily on the amount of liquid electrolyte contained in the dual-layer membrane. Thus, the highest conductivity is obtained at a coating thickness of 0.9 μm, where the electrolyte uptake becomes maximum, as already mentioned in Fig. 4. When the amount of liquid electrolyte contained within the porous polymer matrix

decreases, the number of conducting ions per unit volume lessens and the conduction paths become more tortuous at the same time. On the other hand, if the channels are fully developed and the conduction path is well connected within the dual-layered film as the electrolyte uptake increases, ions can move more promptly through each conduction channel. Thus, the apparent ionic conductivity depends strongly on the electrolyte uptake of the porous polymer matrix.

4. Discharge Behavior of LMPB Unit Cells

Figure 6 shows the initial charge/discharge curves for the Li/dual-layer polymer electrolyte/Li[Ni$_{0.15}$Li$_{0.23}$Mn$_{0.62}$]O$_2$ cells with the various polymer electrolytes cycled between 2.0 and 4.8 V at 25° C. The cells were galvanostatically charged and discharged under a specific current density of 0.5 mA/cm^2 (C/5 rate).
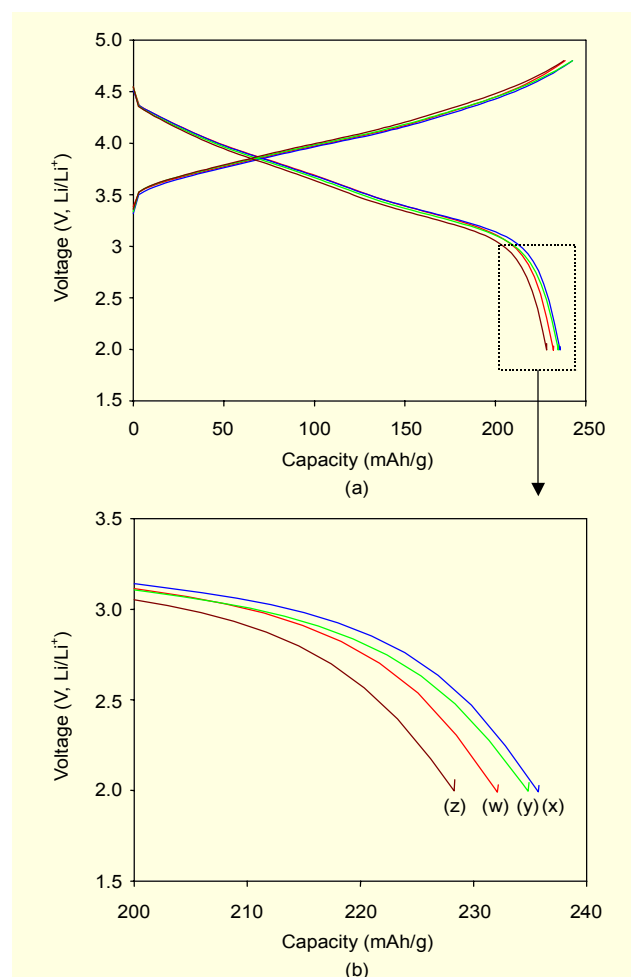

Fig. 6. (a) The initial charge/discharge curves of Li/the dual-layer polymer electrolyte/Li[Ni$_{0.15}$Li$_{0.23}$Mn$_{0.62}$]O$_2$ cells at a C/5 rate (2×2cm^2) and (b) enlarged discharge curves of Fig. 6 (a): (w) a bare PE membrane and (x) 0.9-μm, (y) 6-μm, and (z) 11-μm coated dual-layer polymer electrolytes.

The dual-layer polymer electrolytes with a coated thickness of 0.9 μm, having the largest electrolyte uptake and highest ionic conductivity, give a maximum initial discharge capacity of 236 mAh/g, as (x) in Fig. 6(b) shows. The 11-μm coated membrane, (z) in Fig. 6(b), on the other hand, gives the smallest initial discharge capacity of 228 mAh/g. This may be due to the highest internal cell resistance based on both the decreased conductivity and increased film thickness. In Fig. 7, (z) in the magnified region shows the largest value of intercept

on the real axis (about 16 Ω), which proves that for the 11-μm coated case it has the largest internal resistance value, a sum of the electrolyte resistance (about 6.5 Ω, R_b) and electrolyte/electrode interfacial resistance (diameter of a semicircle, about 9.5 Ω, R_i).

The rechargeability of a unit cell can be evaluated by measuring the decrease in discharge capacities during charge/discharge cycling. The specific discharge capacities of Li/dual-layer polymer electrolyte/Li[$Ni_{0.15}Li_{0.23}Mn_{0.62}$]$O_2$ cells are shown in Fig. 8 as a function of cycle number.

When a bare PE membrane is employed for comparison, the fabricated unit cell has an initial discharge capacity of 232 mAh/g, which decreases to 183 mAh/g after 100 cycles, to 172 mAh/g after 300 cycles, and to 63 mAh/g after 500 cycles, as (w) in Fig. 8 shows. About 21% of its initial discharge capacity is lost during the first 100 cycles, and the remaining capacity is around 27% of its initial value after 500 cycles. Such a significant capacity fade is mainly associated with the interfacial characteristics between the Li anode and the electrolyte films. Since the PE membrane is not compatible with the liquid electrolyte, the gradual leakage of liquid electrolyte from the PE matrix during the cycles would accelerate the dendrite formation and growth to give a large reactive surface area, which leads to the formation of dead Li and an SEI formation on the dendritic anode surface. The formation of voids or the delamination at the interface may reduce the effective contact area between the lithium metal anode and the electrolyte film [5], [16].

However, with the introduction of the coated layer on the PE membrane, the capacity fade of a unit cell can effectively be suppressed and a good cycle performance is realized. At a coating thickness of 11 μm in particular, (z) in Fig. 8, the capacity loss is only 3% after 300 cycles and 13% after 500 cycles. Thus, significant improvement for the cycling performance of the LMPB unit cells can be achieved by introducing a dual-layered porous structure, which is probably due to the smoother electrodeposition of Li$^+$ at the charging stages through the forming of a homogeneous electrolyte zone near the Li-anode surface. To our knowledge, this is the best performance of an LMPB employing a plasticized polymer electrolyte, with excellent mechanical properties and a high ionic conductivity comparable with a usual separator/liquid electrolyte system.
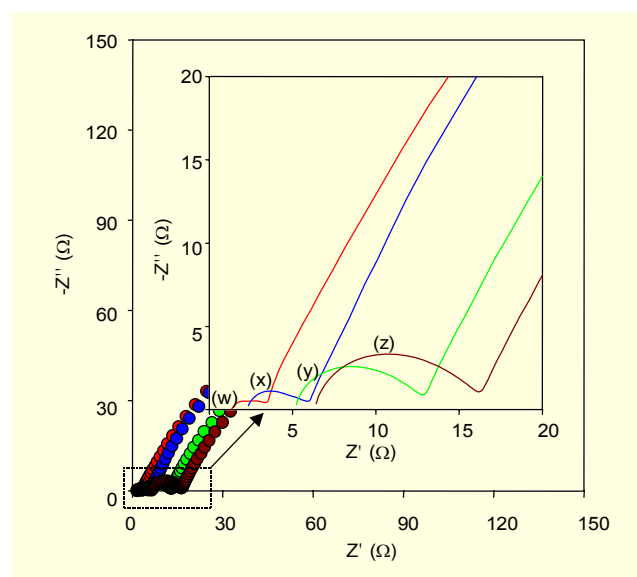

Fig. 7. A typical complex impedance diagram of the unit cells after initial charge/discharge cycle with different dual-layer polymer electrolytes: (w) a bare PE membrane and (x) 0.9-μm, (y) 6-μm, and (z) 11-μm coated dual-layer polymer electrolytes.
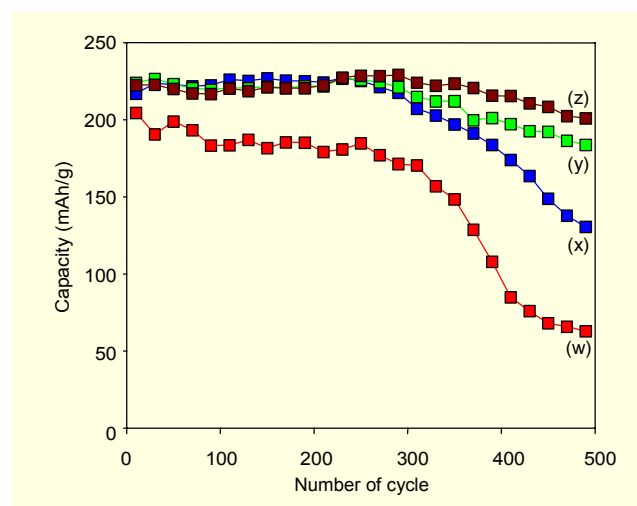

Fig. 8. Discharge capacities of Li/the dual-layer polymer electrolyte/Li[$Ni_{0.15}Li_{0.23}Mn_{0.62}$]$O_2$ cells with a cycle at a C/5 rate: (w) bare PE membrane and (x) 0.9-μm, (y) 6-μm, and (z) 11-μm coated dual-layer polymer electrolytes.

IV. Conclusion

The present study enabled a good cycling performance of an LMPB by applying dual-layered plasticized polymer electrolytes in order to avoid severe dendrite formation and growth during the charging stages. The apparent ionic conductivity of the polymer electrolytes became higher when

increasing the uptake amount of liquid electrolyte into the dual-layered porous matrix. The capacity loss after 500 charge/discharge cycles was successfully reduced to 13% for the optimally fabricated cell.

References

[1] C.A. Vincent and B. Scrosati, *Rechargeable Lithium Cells−Modern Batteries: An Introduction to Electrochemical Power Sources*, Arnold Press, London, 1997.

[2] Y.-S. Hong, K.S. Ryu, and S.H. Chang, "New Iron-Containing Electrode Materials for Lithium Secondary Batteries," *ETRI J.*, vol. 25, no. 5, Oct. 2003, pp. 412-417.

[3] T. Tatsuma, M. Taguchi, M. Iwaku, T. Sotomura, and N. Oyama, "Inhibition Effects of Polyacrylonitrile Gel Electrolytes on Lithium Dendrite Formation," *J. Electroanal. Chem.*, vol. 472, no. 2, Aug. 1999, pp. 142-146.

[4] C. Brissot, M. Rosso, J.N. Chazalviel, and S. Lascaud, "Concentration Measurements in Lithium/Polymer-Electrolyte/Lithium Cells During Cycling," *J. Power Sources*, vol. 94, no. 2, Mar. 2001, pp. 212-218.

[5] Y.G. Lee, J.K. Park, and S.I. Moon, "Interfacial Characteristics between Lithium Electrode and Plasticized Polymer Electrolytes Based on Poly(acrylonitrile-co-methyl methacrylate)," *Electrochim. Acta*, vol. 46, no. 4, Dec. 2000, pp. 533-539.

[6] M. Watanabe, M. Rikukawa, K. Sanui, and N. Ogata, "Effect of Polymer Structure and Incorporated Salt Species on Ionic Conductivity of Polymer Complexes Formed by Aliphatic Polyester and Alkali Metal Thiocyanate," *Macromolecules*, vol. 19, no. 1, Jan. 1986, pp. 188-192.

[7] D. Peramunage, D.M. Pasquariello, and K.M. Abraham, "Polyacrylonitrile-Based Electrolytes with Ternary Solvent Mixtures as Plasticizers," *J. Electrochem. Soc.*, vol. 142, no. 6, June 1995, pp. 1789-1798.

[8] C.H. Kim, H.T. Kim, and J.K. Park, "Novel Electrolyte System: Porous Polymeric Support Filled with Liquid Electrolyte," *J. Appl. Polym. Sci.*, vol. 60, no. 10, June 1996, pp. 1773-1778.

[9] K.M. Kim, J.M. Ko, N.G. Park, K.S. Ryu, and S.H. Chang, "Characterization of Poly(vinylidenefluoride-co-hexafluoropropylene)-Based Polymer Electrolyte Filled with Rutile TiO_2 Nanoparticles," *Solid State Ionics*, vol. 161, no. 1-2, July 2003, pp. 121-131.

[10] F. Croce, L. Persi, F. Ronci, and B. Scrosati, "Nanocomposite Polymer Electrolytes and Their Impact on the Lithium Battery Technology," *Solid State Ionics*, vol. 135, no. 1-4, Nov. 2000, pp. 456-458.

[11] W. Krawiec, L.G. Scanlon Jr., J.P. Fellner, R.A. Vaia, S. Vasudevan, and E.P. Giannelis, "Polymer Nanocomposites: A New Strategy for Synthesizing Solid Electrolytes for Rechargeable Lithium Batteries," *J. Power Sources*, vol. 54, no. 2, Apr. 1995, pp. 310-315.

[12] Y.S. Hong, Y.J. Park, X. Wu, K.S. Ryu, and S.H. Chang, "Synthesis and Electrochemical Properties of Nanocrystalline Li[$Ni_{0.20}Li_{0.20}Mn_{0.60}$]$O_2$," *Electrochem. Solid-State Lett.*, vol. 6, no. 8, Aug. 2003, pp. A166-A169.

[13] Y.J. Park, M.G. Kim, Y.S. Hong, X. Wu, K.S. Ryu, and S.H. Chang, "Electrochemical Behavior of Li Intercalation Processes into a Li[$Ni_xLi_{(1/3-2x/3)}Mn_{(2/3-x/3)}$]$O_2$ Cathode," *Solid State Commun.*, vol. 127, no. 7, Aug. 2003, pp. 509-514.

[14] H. Winkler, "Microstructure of PE-Separators," *J. Power Sources*, vol. 113, no. 2, Jan. 2003, pp. 396-399.

[15] T. Michot, A. Nishimoto, and M. Watanabe, "Electrochemical Properties of Polymer Gel Electrolytes Based on Poly(vinylidenefluoride) Copolymer and Homopolymer," *Electrochim. Acta*, vol. 45, Jan. 2000, pp. 1347-1360.

[16] J.M. Tarascon, A.S. Gozdz, C. Schmutz, F. Shokoohi, and P.C. Warren, "Performance of Bellcore's Plastic Rechargeable Li-ion Batteries," *Solid State Ionics*, vol. 86-88, part 1, July 1996, pp. 49-54.

[17] Y.G. Lee and J.K. Park, "Electrochemical Characteristics of Polymer Electrolytes Based on P(VdF-co-HFP)/PMMA Ionomer Blend for PLIB," *J. Power Sources*, vol. 97-98, July 2001, pp. 616-620.

[18] F. Orsini, A.D. Pasquier, B. Beaudoin, J.M. Tarascon, M. Trentin, N. Langenhuizen, E. De Beer, P. Notten, "In Situ Scanning Electron Microscopy (SEM) Observation of Interfaces within Plastic Lithium Batteries," *J. Power Sources*, vol. 76, no. 1, Nov. 1998, pp. 19-29.

Young-Gi Lee received the BS degree in chemical engineering from Pusan National University, Korea, in 1995 and the MS and PhD degrees in polymer materials and chemistry from Korea Advanced Institute of Science and Technology (KAIST) in Daejeon, Korea, in 1997 and 2001. He joined Basic Research Laboratory at the Electronics and Telecommunications Research Institute (ETRI) in 2001 and has been working in the Ionics Devices Team. His research topics are polymer electrolytes for lithium metal polymer batteries, separators for lithium-ion batteries, ion exchange membranes for polymer electrolyte fuel cells and direct methanol fuel cells, surface modification of inorganic fillers, and modification of lithium metal surfaces.

Kwang Sun Ryu received the BS and MS degrees in chemistry from Yonsei University, Seoul, Korea in 1986 and 1990, and his PhD degree in polymer physical chemistry from Yonsei University in 1996. From 1996 to 1997, he was a Post-Doctorial Researcher in ETRI and Tokyo University of Arg. & Tech (TUAT). Since he joined ETRI in 1998, he has worked in Ionics Devices Team. His current topics of interest are conducting polymers, polymer physical properties, nano-polymer technology, lithium secondary batteries, and supercapacitors.

Soon Ho Chang received the BS and MS degrees in chemistry from Yonsei University, Korea, in 1982 and the PhD degree for research in intercalation/deintercalation in inorganic compounds from Bordeaux University in France in 1989. He has been working in Ionics Devices Team of ETRI since 1990. From 2002 to 2003, he was in charge of Applied Device Department at the Basic Research Laboratory.